Trajectory and force control of a manipulator with elastic links

Katsuyoshi Tsujita ,Kazuo Tsuchiya ,Takateru Urakubo and Zenta Sugawara

Dept. of Aeronautics and Astronautics, Graduate School of Engineering, Kyoto University

Yoshida-Hon-Machi, Sakyo-ku, Kyoto 606-8501, Japan

E-mail : tsujita@kuaero.kyoto-u.ac.jp

Phone: +81-774-38-3961 Facsimile: +81-774-38-3962

Abstract

This article deals with trajectory and force control of a two-link manipulator with elastic links. The manipulator has a macro-micro mechanism and at the tip of which has a end effector with a force sensor. Equations of motion are first derived by using a finite element method for the elastic deformations and then by eliminating the residual modes based on the eigen value analysis, the reduced order equations for controller design are derived. Geometrical constraints are modeled by using Lagrangian multiplier. The proposed control system consists of feedforward controller and feedback controller. The feedforward controller generates the input torques and force based on inverse dynamics. It also generates the reference signals for the feedback controller based on inverse kinematics. The calculation methods for inverse dynamics and inverse kinematics are based on the algorithm which the authors have proposed. Performance of the proposed control system is verified by numerical simulations and hardware experiments.

Keywords: Manipulator, Elastic link, Trajectory and force control, Micro-macro mechanism

1 Introduction

A manipulator is a mechanical system whose links are connected through translational or rotational joints. A manipulator is called a flexible manipulator when the elastic deformations of the links cannot be ignored. One of the tasks for the manipulator is a manipulation of an object. This task is established by controlling the force acting on the object from the end effector of the manipulator. Usually, the manipulation task has not been given for the flexible manipulator because it has not been expected a good performance because of the disturbances of the elastic deformations. But the flexible manipulator has an advantage on the manipulation task that it degrades the shock force of the collision with the object because of its elastic deformations. Therefore, a considerable amount of research has been started on the design of controllers for manipulation task of the flexible manipulators. In this article, trajectory and force controller of a flexible manipulator is proposed. From the point of view of structural dynamics, trajectory control for a flexible manipulator is to control the global elastic deformation of the system, and force control of a flexible manipulator is to control the local deformation at the tip of the end effector. Then, it is preferred that trajectory control and force control are separated. In this work, for this end, the authors treated a manipulator at the tip of which has a small end effector. The end effector has two degrees of freedom for force control and at the tip of which is mounted a force sensor. This type of manipulator is called a macro-micro manipulator.

Trajectory and force control of the flexible manipulator is required to control the local dynamic deformation at the end of the manipulator. From the previous researches for motion control of the flexible manipulator, it has become clear that using only a feedback controller is not always expected to be effective for motion control, and then, a considerable amount of researches has been done on motion control of flexible manipulators by utilizing feedforward

control. Feedforward control includes two inputs: One is the command signals of feedforward force/torque which are served to the actuator as the control input. The other is the reference signals of the state variable which are served to the feedback controller. The former is computed based on inverse dynamics and the latter is computed based on inverse kinematics. In this article, a control system for trajectory and force control of a flexible manipulator is proposed which consists of feedforward controller and feedback controller. Most algorithms for inverse dynamics and inverse kinematics which have proposed so far are iteration methods and have a problem on convergence of solutions. The authors have proposed an algorithm for inverse kinematics and inverse dynamics in which the equations of the elastic deformations of the links are reformulated as boundary value problems. This algorithm is one shot calculation method, which has no problem on convergence of the solutions.

Performance of the trajectory and force controller has a strong influence with the friction in the mechanism of the manipulator or between the end effector and the surface of the handling object. But it is not realistic to derive the model of the friction neither to consider it for design of the control system, because the friction has a large variance depending on various situations and it is too difficult to identify the parameters of the friction. Therefore, the proposed control system has no heuristic information on the friction. The effect of the friction is investigated by numerical simulations and hardware experiments.

2 Model

In this section, equations of motion of the manipulator are derived. The manipulator consists of four bodies (Figure 1). Bodies 1,3 and 4 are rigid rods and body 2 is an elastic beam, whose elastic deformation occurs in a plane perpendicular to the rotational axis. Body 1 is put on a base-mount with a rotational joint (joint 1) and bodies from 1 to 3, in this turn, are connected to

the next through rotational joints. Body 4 is connected to body 3 through a translational joint. Rotational actuators are installed at joints 1, 2, 3 and the axes of which are perpendicular to a sagittal plane. Translational actuator is installed at joint 4 and moves linearly in the sagittal plane.

Several dynamic models of constrained flexible manipulator have been proposed. The modeling method in this work is as follows: The elastic deformation of body 2 is modeled by using finite element method. Since the derived equations of motion become to be high dimensional equations, the reduced dimensional equations are required for controller design, which are derived in section 3. The geometric constraints in the direction of normal vector of the surface of the object are formulated by using Lagrangian multiplier method. In tangent direction of the surface of the object, the model of friction between the end of the manipulator and the surface of the object is formulated combining the static friction and viscous friction.

Introduce a set of unit vectors $\{\boldsymbol{a}^{(0)}\} = \{\boldsymbol{a}_1^{(0)}, \boldsymbol{a}_2^{(0)}, \boldsymbol{a}_3^{(0)}\}$ fixed in an inertia space, the origin of which coincides with joint 1. Vector $\boldsymbol{a}_3^{(0)}$ coincides with the axis of rotation and vector $\boldsymbol{a}_2^{(0)}$ is set downward. A set of unit vectors $\{\boldsymbol{a}^{(i)}\} = \{\boldsymbol{a}_1^{(i)}, \boldsymbol{a}_2^{(i)}, \boldsymbol{a}_3^{(i)}\}$ is introduced, the origin of which coincides with joint i $(i = 1, 2, 3)$. Vector $\boldsymbol{a}_3^{(i)}$ coincides with the axis of rotation of joint i and vector $\boldsymbol{a}_1^{(i)}$ is set toward the axis of body i. Using a set of unit vectors $\{\boldsymbol{a}^{(i)}\}$, following matrix is introduced,

$$[\boldsymbol{a}^{(i)}]^T = [\boldsymbol{a}_1^{(i)}, \boldsymbol{a}_2^{(i)}, \boldsymbol{a}_3^{(i)}] \tag{1}$$

By introducing the angles of rotation from $\{\boldsymbol{a}^{(j)}\}$ to $\{\boldsymbol{a}^{(i)}\}$ about $\boldsymbol{a}_3^{(i)}$ axis as $\theta_3^{(ij)}$, transformation matrices from $\{\boldsymbol{a}^{(j)}\}$ to $\{\boldsymbol{a}^{(i)}\}$ are defined by $A^{(ij)}$.

The angular velocity vector of $\{\boldsymbol{a}^{(i)}\}$ to $\{\boldsymbol{a}^{(j)}\}$ is defined by $\boldsymbol{\omega}^{(ij)}$

$$\begin{aligned} \boldsymbol{\omega}^{(ij)} &= [\boldsymbol{a}^{(i)}]^T \omega^{(ij)} \\ \omega^{(ij)T} &= [\ 0,\ 0,\ \dot{\theta}_3^{(ij)}\ ] \end{aligned} \tag{2}$$

The following quantities are introduced,

$\boldsymbol{r}^{(i)} = [\boldsymbol{a}^{(i)}]^T r^{(i)}$; a distance vector from joint i to joint $i+1$ ($i = 1,\ 2$).

$\boldsymbol{R}^{(i)} = [\boldsymbol{a}^{(i)}]^T R^{(i)}$; a distance vector from joint i to C.M. (center of mass) of body i.

$\boldsymbol{r}_c^{(4)} = [\boldsymbol{a}^{(3)}]^T r_c^{(4)}$; a distance vector from joint 3 to C.M. of body 4.

$\boldsymbol{r}^{(4)} = [\boldsymbol{a}^{(3)}]^T r^{(4)}$; a distance vector from joint 3 to the end effector.

$\boldsymbol{r}_e^{(4)} = [\boldsymbol{a}^{(3)}]^T r_e^{(4)}$; a distance vector from C.M. of body 4 to the end effector.

$$(\boldsymbol{r}_e^{(4)} = \boldsymbol{r}^{(4)} - \boldsymbol{r}_c^{(4)})$$

$\boldsymbol{\rho}^{(i)} = [\boldsymbol{a}^{(i)}]^T \rho^{(i)}$; a distance vector from joint i to any position in body i.

The elastic deformation of body 2 is denoted by $\boldsymbol{w}^{(2)}$.

$$\begin{aligned} \boldsymbol{w}^{(2)} &= [\boldsymbol{a}^{(2)}]^T w^{(2)} \\ w^{(2)T} &= [0,\ w_2^{(2)}(t,\ \rho_1^{(2)}),\ 0] \end{aligned} \tag{3}$$

The elastic deformation of body 2 is modeled by using finite element method. (See appendix) Body 2 is divided into N finite elements, which are numbered as 1, 2, $\cdots$, N from joint 2 to joint 3. The nodes are also numbered as 0, 1, $\cdots$, N from joint 2 to joint 3. Joint 2 and 3 are nodes 0 and N, respectively. The elastic deformation $w_2^{(2)}(t,\ \rho_1^{(2)})$ is expressed as

$$w_2^{(2)}(t,\ \rho_1^{(2)}) = B^{(2)}(\rho_1^{(2)})\hat{w}_2^{(2)}(t) \tag{4}$$

$$\begin{aligned} \widehat{w}_2^{(2)T} &= \Big[\widehat{w}_{2,1}^{\prime(2)}\ ,\ \widehat{w}_{2,2}^{(2)}\ ,\ \widehat{w}_{2,2}^{\prime(2)}\ , \\ &\qquad \cdots\ ,\ \widehat{w}_{2,N-2}^{(2)}\ ,\ \widehat{w}_{2,N-2}^{\prime(2)}\ ,\ \widehat{w}_{2,N-1}^{(2)}\Big] \end{aligned}$$

where $\widehat{w}_{2,n}^{(2)}$ and $\widehat{w}_{2,n}^{\prime(2)}$ are the elastic deformation and the angle of rotation at node n, respectively. At nodes 0 and N, we may set the following condition;

$$\widehat{w}_{2,0}^{(2)} = \widehat{w}_{2,N}^{(2)} = 0$$

A state variables z of the system are set to be

$$z^T = \left[\theta_3^{(10)},\ \theta_3^{(21)},\ \hat{w}_2^{(2)T},\ \theta_3^{(30)},\ r_{c2}^{(4)} \right] \tag{5}$$

The equations of motion for state variables z are derived as follows;

$$\begin{aligned}
&\frac{d}{dt}\left\langle \tilde{\rho}_c^{(1)T} v^{(1)} \right\rangle^{(1)} + \left\langle \tilde{\rho}_c^{(1)T} \tilde{\omega}^{(10)T} v^{(1)} \right\rangle^{(1)} \\
&= -\tilde{r}_c^{(1)T} f^{(1)} - (\tilde{r}^{(1)T} - \tilde{r}_c^{(1)T}) A^{(12)} f^{(2)} \\
&\qquad + \tau^{(1)} - A^{(12)} \tau^{(2)}
\end{aligned} \tag{6}$$

$$\begin{aligned}
&\frac{d}{dt}\left\langle \tilde{\rho}_c^{(2)T} v^{(2)} \right\rangle^{(2)} + \left\langle \tilde{\rho}_c^{(2)T} \tilde{\omega}^{(20)T} v^{(2)} \right\rangle^{(2)} \\
&= -\tilde{r}_c^{(2)T} f^{(2)} - (\tilde{r}^{(2)T} - \tilde{r}_c^{(2)T}) A^{(23)} f^{(3)} \\
&\qquad + \tau^{(2)} - A^{(23)} \tau^{(3)}
\end{aligned} \tag{7}$$

$$\begin{aligned}
&\frac{d}{dt}\left\langle \tilde{\rho}_c^{(3)T} v^{(3)} \right\rangle^{(3)} + \left\langle \tilde{\rho}_c^{(3)T} \tilde{\omega}^{(30)T} v^{(3)} \right\rangle^{(3)} \\
&= -\tilde{r}_c^{(3)T} f^{(3)} - (\tilde{r}^{(3)T} - \tilde{r}_c^{(3)T}) A^{(34)} f^{(4)} + \tau^{(3)}
\end{aligned} \tag{8}$$

$$\begin{aligned}
&\frac{d}{dt}\left\langle v^{(4)} \right\rangle^{(4)} + \tilde{\omega}^{(40)T} \left\langle v^{(4)} \right\rangle^{(4)} \\
&= f^{(4)} - m^{(4)} A^{(40)} g + A^{(40)} f^{(e)}
\end{aligned} \tag{9}$$

where $v^{(i)}$ is the linear velocity of C.M. of body i and $\tilde{*}$ is the cross product.

The equations for variables $\theta_3^{(10)}$,$\theta_3^{(21)}$, $\theta_3^{(32)}$ are derived from the equations of the momenta of bodies. Equation (6) is that of total angular momentum of bodies 1 through 4 at joint 1, equation (7) is that of angular momentum of the subsystem, bodies 2 through 4, at joint 2, equation (8) is that of angular momentum of the subsystem, bodies 3 and 4, at joint 3 and equation (9) is that of linear momentum of body 4.

In addition, equations of motion for variable $\hat{w}_2^{(2)}$ are derived from the equations of elastic

deformation of body 2 as follows;

$$\begin{aligned}
&\frac{d}{dt}\left\langle B^{(2)T}v^{(2)}\right\rangle^{(2)} + \left\langle B^{(2)T}\tilde{\omega}^{(20)T}v^{(2)}\right\rangle^{(2)} \\
&\qquad +K^{(2)}\widehat{w}^{(2)} + D^{(2)}\widehat{w}^{(2)} \\
&= \left\langle B^{(2)T}\right\rangle^{(2)} A^{(20)}g \\
&\qquad -B^{(2)T}(r^{(2)})A^{(23)}f^{(3)} \\
&\qquad +E_1^{(2)T}\tau_3^{(2)} + E_2^{(2)T}\tau_3^{(3)}
\end{aligned} \tag{10}$$

where,

$$\begin{aligned}
\rho_c^{(i)} &= \rho^{(i)} - r_c^{(i)}\ ,\ r_c^{(i)} = \frac{1}{m^{(i)}}\int \rho^{(i)}dm^{(i)} \\
< * >^{(i)} &= \int *dm^{(i)} \\
E_1^{(2)} &= \left[\begin{array}{ccccc} 1 & 0 & \cdots & 0 & 0 \end{array}\right] \\
E_2^{(2)} &= \left[\begin{array}{ccccc} 0 & 0 & \cdots & 0 & 1 \end{array}\right]
\end{aligned}$$

$m^{(i)}$ is mass of body i, $\boldsymbol{f}^{(i)} = [\boldsymbol{a}^{(i)}]^T f^{(i)}$ and $\boldsymbol{\tau}^{(i)} = [\boldsymbol{a}^{(i)}]^T \tau^{(i)}$ are force and torque acting on body i at joint i. $\boldsymbol{f}^{(e)} = [\boldsymbol{a}^{(0)}]^T f^{(e)}$ is force acting on the surface of the object through the end effector.

The forces $f^{(i)}$ $(i = 1, \cdots, 4)$ are expressed as

$$\begin{aligned}
f^{(1)} &= \frac{d}{dt}\left\langle v^{(1)} \right\rangle^{(1)} + \tilde{\omega}^{(10)T}\left\langle v^{(1)} \right\rangle^{(1)} \\
&\quad -m^{(1)}A^{(10)}g + A^{(12)}f^{(2)} \\
f^{(2)} &= \frac{d}{dt}\left\langle v^{(2)} \right\rangle^{(2)} + \tilde{\omega}^{(20)T}\left\langle v^{(2)} \right\rangle^{(2)} \\
&\quad -m^{(2)}A^{(20)}g + A^{(20)}f^{(e)} \\
f^{(3)} &= \frac{d}{dt}\left\langle v^{(3)} \right\rangle^{(3)} + \tilde{\omega}^{(30)T}\left\langle v^{(3)} \right\rangle^{(3)} \\
&\quad -m^{(3)}A^{(30)}g + A^{(30)}f^{(4)} \\
f^{(4)} &= \frac{d}{dt}\left\langle v^{(4)} \right\rangle^{(4)} + \tilde{\omega}^{(40)T}\left\langle v^{(4)} \right\rangle^{(4)} \\
&\quad -m^{(4)}A^{(40)}g + A^{(40)}f^{(e)}
\end{aligned} \tag{11}$$

where g is a gravitational constant.

The surface curve of the target object is modeled as $[\boldsymbol{a}_0]^T\Phi$. The geometric constraint of the tip of the manipulator in the normal direction of the surface is formulated as follows;

$$\Phi = A^{(01)}r^{(1)} + A^{(02)}r^{(2)} + A^{(03)}r^{(3)} + A^{(04)}r^{(4)}$$

On the other hand, the model of friction between the tip of the manipulator and the surface of the object in tangent direction is formulated as follows;

$$\begin{aligned}
&F_t = \boldsymbol{i}_t^T \boldsymbol{f}^{(e)} \\
&= \begin{cases} -f_0 \ sgn(\boldsymbol{i}_t^T \dot{x}^{(e)}) - \nu \ \boldsymbol{i}_t^T \dot{x}^{(e)}; & |\boldsymbol{i}_t^T \dot{x}^{(e)}| > \epsilon \\ (\text{constrained}); & \boldsymbol{i}_t^T \boldsymbol{f}^{(e)} \leq \mu \ \boldsymbol{i}_n^T \boldsymbol{f}^{(e)}, |\boldsymbol{i}_t^T \dot{x}^{(e)}| \leq \epsilon \end{cases}
\end{aligned}$$

$\boldsymbol{i}_t$: tangent vector of the surface of the object

$\boldsymbol{i}_n$: normal vector of the surface of the object

f_0 : bias friction force

ν : coefficient of viscous friction

μ : coefficient of maximum static friction

3 Control system

This section deals with design of the control system for trajectory and force control of the manipulator.

3.1 Basic equations

Reduced dimensional equations are derived as follows: At first, a nominal posture of the manipulator is determined corresponding to the manipulating situation. Motion of joint 1 is fixed to the nominal position. The motion trajectories of joint 2 through 4 are controlled by appropriate feedback control using the nominal values as reference signals. The equations of motion are linearized around the nominal values corresponding to the given nominal posture of the manipulator. By analyzing the eigen values of the linearized equations, the modes are picked up as the controlled modes which have low natural frequency and have large effects on the position of the end of the manipulator. The reduced dimensional equations are composed of the controlled modes.

Variables $\widehat{w}_2^{(2)}$,$v^{(2)}$ are expressed as follows;

$$
\begin{aligned}
\widehat{w}_2^{(2)} &= Uq \\
q^T &= [q_1,\ \cdots,\ q_m] \\
v^{(2)} &= A^{(21)}\tilde{r}^{(1)}{}_{\omega}{}^{(10)} \\
&\quad + \left\{ \tilde{\rho}^{(2)}\omega^{(20)} + B^{(2)}(\rho_1^{(2)})U\dot{q} \right\} \\
m &: \text{number of controlled modes}
\end{aligned}
$$

where, U is composed of eigen vectors of $< B^{(2)T}B^{(2)} >^{(2)^{-1}} K^{(2)}$, and satisfies following conditions.

$$
\begin{aligned}
U &= [\ e_1\ e_2\ \cdots\ e_m\ ] \\
e_i &: \text{eigen vector of} < B^{(2)T} B^{(2)} >^{(2)^{-1}} K^{(2)} \quad (\ i = 1,\ 2,\ \cdots, m\ )
\end{aligned}
$$

Equation (10) is alternated as following one by substituting $\widehat{w}_2^{(2)}$ into equation (10);

$$
\begin{aligned}
&\frac{d}{dt}\left\langle U^T B^{(2)T} v^{(2)} U \right\rangle^{(2)} + U^T \left\langle B^{(2)T} \tilde{\omega}^{(20)T} v^{(2)} \right\rangle^{(2)} U \\
&\qquad + U^T K^{(2)} U q + U^T D^{(2)} U q \\
&= U^T \left\langle B^{(2)T} \right\rangle^{(2)} A^{(20)} g \\
&\qquad - U^T B^{(2)T} (r^{(2)}) A^{(23)} f^{(3)} \\
&\qquad + U^T E_1^{(2)T} \tau_3^{(2)} + U^T E_2^{(2)T} \tau_3^{(3)}
\end{aligned} \tag{12}
$$

3.2 Controller

The proposed control system consists of feedforward controller and feedback controller. The feedforward controller generates the input torque and force based on inverse dynamics. And it also generates the reference signals for the feedback controller based on inverse kinematics[16]. At first, inverse kinematics is implemented as follows: A desired trajectory $\boldsymbol{x}_d^{(e)}(t) = [\boldsymbol{a}^{(0)}]^T x_d^{(e)}$ of the end effector and desired force $\boldsymbol{f}_d^{(e)}(t) = [\boldsymbol{a}^{(0)}]^T f_d^{(e)}$ acting on the surface of the object through the end effector are given as functions of time t.

$$
\begin{aligned}
\boldsymbol{x}_d^{(e)} &= [\boldsymbol{a}^{(0)}]^T x_d^{(e)}(t) \\
\boldsymbol{f}_d^{(e)} &= [\boldsymbol{a}^{(0)}]^T f_d^{(e)}(t)
\end{aligned} \tag{13}
$$

The nominal position and posture of body 4 are given as

$$
\begin{aligned}
r_{cd2}^{(4)} &= \text{const.} \\
\theta_{d3}^{(30)} &= \tan^{-1}\left(\frac{\partial x_{d2}^{(e)}}{\partial x_{d1}^{(e)}}\right)
\end{aligned} \tag{14}
$$

Under the condition of equation (14), equation (13), we obtain the equation to determine the angles of rotation $\theta_{d3}^{(10)}$, $\theta_{d3}^{(21)}$.

$$\begin{aligned} x_{d1}^{(e)}(t) = \; & r^{(1)}\cos\theta_{d3}^{(10)} + r^{(2)}\cos\theta_{d3}^{(20)} \\ & + r_{c1}^{(4)}\cos\theta_{d3}^{(30)} - (r_{cd2}^{(4)} + r_e^{(4)})\sin\theta_{d3}^{(30)} \\ x_{d2}^{(e)}(t) = \; & r^{(1)}\sin\theta_{d3}^{(10)} + r^{(2)}\sin\theta_{d3}^{(20)} \\ & + r_{c1}^{(4)}\sin\theta_{d3}^{(30)} + (r_{cd2}^{(4)} + r_e^{(4)})\cos\theta_{d3}^{(30)} \end{aligned} \tag{15}$$

Next, substituting the desired force $f_d^{(e)}(t)$ and the obtained angles of rotation $\theta_{d3}^{(10)}(t)$, $\theta_{d3}^{(21)}(t)$ into equation (10), we obtain the equation to determine the elastic deformations $q_d(t)$.

$$\begin{aligned} & \widehat{M}^{(2)}\ddot{q}_d + \left\{\widehat{K}^{(2)} - \omega_{d3}^{(20)2}\widehat{M}^{(2)}\right\} q_d \\ & \quad = \left(-g_2\cos\theta_{d3}^{(20)} - r_1^{(1)}\omega_{d3}^{(10)2}\sin\theta_{d3}^{(21)} - r_1^{(1)}\dot{\omega}_{d3}^{(10)}\cos\theta_{d3}^{(21)}\right) U^T < B_2^{(2)T} >^{(2)} \\ & \qquad -\dot{\omega}_{d3}^{(20)} U^T < B_2^{(2)T}\rho_1^{(2)} >^{(2)} + Q_1 U^T E_1^{(2)T} + Q_2 U^T E_2^{(2)T} \end{aligned} \tag{16}$$

$$\begin{aligned} Q_2 = \; & r_1^{(1)}\left\{(m^{(3)}r_{c1}^{(3)} + m^{(4)}r_{cd1}^{(4)})\cos\theta_{d3}^{(31)} - (m^{(3)}r_{c2}^{(3)} + m^{(4)}r_{cd2}^{(4)})\sin\theta_{d3}^{(31)}\right\}\dot{\omega}_{d3}^{(10)} \\ & + r_1^{(2)}\left\{(m^{(3)}r_{c1}^{(3)} + m^{(4)}r_{cd1}^{(4)})\cos\theta_{d3}^{(32)} - (m^{(3)}r_{c2}^{(3)} + m^{(4)}r_{cd2}^{(4)})\cos\theta_{d3}^{(31)}\right\}\dot{\omega}_{d3}^{(20)} \\ & + (J^{(3)} + J^{(4)})\dot{\omega}_{d3}^{(30)} \end{aligned}$$

$$\begin{aligned} Q_1 = \; & Q_2 \\ & + r_1^{(1)}\left\{m^{(2)}r_{c1}^{(2)} + (m^{(3)} + m^{(4)})r_1^{(2)}\right\}\cos\theta_{d3}^{(21)}\dot{\omega}_{d3}^{(10)} \\ & + \left\{(m^{(3)}r_{c1}^{(3)} + m^{(4)}r_{cd1}^{(4)})\cos\theta_{d3}^{(32)} - (m^{(3)}r_{c1}^{(3)} + m^{(4)}r_{cd2}^{(4)})\sin\theta_{d3}^{(32)}\right\}\dot{\omega}_{d3}^{(30)} \\ & + \omega_{d3}^{(10)2} r_1^{(2)}\left\{(m^{(2)}r_{c1}^{(2)} + (m^{(3)} + m^{(4)})r_1^{(2)}\right\}\sin\theta_{d3}^{(21)} \\ & - \omega_{d3}^{(30)2} r_1^{(2)}\left\{(m^{(3)}r_{c1}^{(3)} + m^{(4)}r_{cd1}^{(4)})\sin\theta_{d3}^{(32)} + (m^{(3)}r_{c2}^{(3)} + m^{(4)}r_{cd2}^{(4)})\cos\theta_{d3}^{(32)}\right\} \\ & + \left\{m^{(2)}r_{c1}^{(2)} + (m^{(3)} + m^{(4)})r_1^{(2)}\right\} g_2\cos\theta_{d3}^{(20)} \\ & + f_{d1}^{(e)} r_1^{(2)}\sin\theta_{d3}^{(20)} - f_{d2}^{(e)} r_1^{(2)}\cos\theta_{d3}^{(20)} \end{aligned}$$

$$\widehat{M}^{(2)} = U^T < B_2^{(2)T} B_2^{(2)} >^{(2)} U - U^T < E^{(2)T} C^{(2)} >^{(2)} U$$

$$\widehat{K}^{(2)} = U^T K^{(2)} U$$

where, $C^{(2)} = [< \rho_1^{(2)} B_2^{(2)} >^{(2)},\ 0,\ \cdots,\ 0\ ]$.

Equation (16) is a set of second order ordinary differential equations and is to be formulated as an initial value problem with the initial conditions as

$$t = 0, \qquad q_d = \dot{q}_d = 0$$

However, since the coefficient matrix of $\ddot{q}_d$ is not positive definite, equation (16) is not well posed as an initial value problem. Here, equation (16) is formulated as boundary value problem with the boundary conditions

$$\begin{array}{ll} t = 0 & q_d = \hat{q}_{d,i} \\ t = t_f & q_d = \hat{q}_{d,f} \end{array} \tag{17}$$

where, t_f is a time interval of manipulation, and $\hat{q}_{d,i}$, $\hat{q}_{d,f}$ are values of static deformations in the initial and final configurations.

As boundary value problems, we can obtain a stable solution numerically, but the elastic deformation q_d obtained has certain velocity at the beginning of manipulation. This velocity is affected by smoothness of acceleration in initial state. Therefore, the appropriate trajectory $\boldsymbol{x}_d^{(e)}(t)$ should be given as sufficiently smooth acceleration.

When the angle of rotation $\theta_{d3}^{(10)}(t)$ and $\theta_{d3}^{(21)}(t)$ and elastic deformation $q_d(t)$ are obtained by inverse kinematics, inverse dynamics is used to calculate the input force $f_d^{(4)}(t)$ which realize the desired motion.

Input force $f_d^{(4)}(t)$ is calculated by using equations (6) and (7).

Here, $f_d^{(4)}(t)$ is expressed as follows;

$$\begin{aligned} f_{d2}^{(4)} = m^{(4)} \Big(& r_1^{(1)} \ddot{\theta}_{d3}^{(10)} \cos\theta_{d3}^{(31)} + r_1^{(2)} \ddot{\theta}_{d3}^{(20)} + r_{c1}^{(4)} \ddot{\theta}_{d3}^{(30)} + \dot{\theta}_{d3}^{(10)2} r_1^{(1)} \sin\theta_{d3}^{(31)} + \dot{\theta}_{d3}^{(20)2} r_1^{(2)} \sin\theta_{d3}^{(32)} \\ & - \dot{\theta}_d^{(30)2} r_{cd2}^{(4)} \Big) + m^{(4)} g \cos\theta_{d3}^{(30)} + f_{d1}^{(e)} \sin\theta_{d3}^{(30)} - f_{d2}^{(e)} \cos\theta_{d3}^{(30)} \end{aligned} \tag{18}$$

By using the above result, the input commands to the motors at the joints are designed as

follows;

$$\tau_c^{(1)} = K_p^{(1)}(\theta_{d3}^{(10)} - \theta_3^{(10)}) + K_d^{(1)}(\dot{\theta}_{d3}^{(10)} - \dot{\theta}_3^{(10)}) \tag{19}$$

$$\tau_c^{(2)} = K_p^{(2)}(\phi_{d3}^{(21)} - \phi_3^{(21)}) + K_d^{(2)}(\dot{\phi}_{d3}^{(21)} - \dot{\phi}_3^{(21)}) \tag{20}$$

$$\tau_c^{(3)} = K_p^{(3)}(\theta_{d3}^{(30)} - \theta_3^{(30)}) + K_d^{(3)}(\dot{\theta}_{d3}^{(30)} - \dot{\theta}_3^{(30)}) \tag{21}$$

$$f_c^{(4)} = f_{d2}^{(4)} + K_p^{(4)}(f_2^{(e)} - f_{d2}^{(e)}) + K_i^{(4)} \int (f_2^{(e)} - f_{d2}^{(e)})dt \tag{22}$$

$$\phi_2^{(21)} = \theta_2^{(21)} + E_1^{(2)} U q \tag{23}$$

Feedback gains are determined as follows: First, consider deviations of variables $f_2^{(e)}$, q, and the derivatives of them from the nominal values.

$$\begin{aligned} z &= z^* + \Delta z \\ \dot{z} &= \dot{z}^* + \Delta \dot{z} \\ f_2^{(e)} &= f_{d2}^{(e)} + \Delta f_2^{(e)} \end{aligned} \tag{24}$$

Following vector is defined.

$$X = \left[\begin{array}{ccc} \Delta \dot{z} & \Delta z & \displaystyle\int_0^t \Delta f_2^{(e)} dt \end{array} \right]^T \tag{25}$$

Substituting equation (24) into equations (6), (7) and (10) to linearize them, following equations are obtained.

$$\dot{X} = H_1(t)X + H_2(t) \tag{26}$$

Equation (26) is a linear ordinary differential equation which has time variant coefficients. Feedback gains are determined by analyzing the eigen values of the equation considering time t in the coefficient as a parameter.

4 Numerical simulation and hardware experiment

The proposed control system is designed based on the reduced dimensional model and uses no a priori information about properties of the mechanical friction nor the friction between the end

of the manipulator and the surface of the object. The influences of the friction to performance of the proposed control system and instability of spillover are verified by numerical simulations and hardware experiments. The values of parameters of the manipulator are listed in Table 1.

Figure 2 shows the result of eigenvalue analysis in order to derive the reduced dimensional equations mentioned in section 3. The horizontal axis is frequency and the vertical axis is normalized position of the end of the manipulator. The reduced dimensional equations for design of the control system include from 1st to 3rd modes. While the reduced dimensional equations for numerical simulation include from 1st to 6th modes.

Desired trajectory of the end effector, $\boldsymbol{x}_d^{(e)}(t)$, and the desired force acting on the surface, $\boldsymbol{f}_d^{(e)}$, are given as follows;

$$
\begin{aligned}
f_{d2}^{(e)}(t) &= 10.0 \quad [\mathrm{N}] \\
x_{d1}^{(e)}(t) &= 0.67 - 0.22(-252\hat{t}^{11} + 1386\hat{t}^{10} - 3080\hat{t}^{9} + 3465\hat{t}^{8} - 1980\hat{t}^{7} + 462\hat{t}^{6}) \quad [\mathrm{m}]
\end{aligned}
$$

$$
x_{d2}^{(e)} = \begin{cases} -0.077 \quad [\mathrm{m}] & (CASE\ 1) \\ -0.077 - \sqrt{0.625^2 - (x_{d1}^{(e)}(t) - 0.67)^2}\ [\mathrm{m}] & (CASE\ 2) \end{cases}
$$

where, $\hat{t} = t/t_f$, $t_f = 2.0$ [sec].

The surface in CASE 1 is a flat horizontal plane below the height of joint 1 and that in CASE 2 is a part of circular cylinder.

At first, performance of the proposed control system is verified by numerical simulations. Figures 3(a),3(b) are the effects of friction on performance of the control system. In figure 3(a), horizontal axis is desired contact force $f_{d2}^{(e)}$ and vertical axis is the error of the controlled contact force. Figure 3(b) is a magnified figure of figure 3(a). From these figures, it is found that the friction between the end of the manipulator and the surface of the object has a strong effect on accuracy of motion control, while the mechanical friction at joint 4 has a strong effect on force

control.

Figure 4 indicates the time history of the contact force acting on the surface of the object in CASE 1. Figure 5 are the results of CASE 2. The properties of friction are identified by experiments in advance. In the figures, solid line is the result of the case that two types of friction are taken into consideration, friction between the end effector and the surface of the object, and that of linear actuator, joint 4. Dashed line is the result of the case that there is not friction of the linear actuator, joint 4, but friction model between the end effector and the surface of the object.

The peak errors in figures 4(b) and 5(b) are due to the effects of stick-slip caused by the mechanical friction at joint 4. While the peak errors in figures. 4(a) and 5(a) are due to the effects of stick-slip caused by the frictions between the end of the manipulator and the surface of the object.

Next, performances of the proposed controller are also verified by hardware experiments.

Figure 6 shows the hardware equipment. Figure 7 shows the architecture of the hardware equipment. Figures 8 and 9 show the results of hardware experiments. These figures express the time history of the measured reaction force at the end effector. Actually, it was difficult to measure the position errors of the end effector accurately by using the hardware equipment. From figures 8 and 9, due to the friction of joint 4 (linear actuator), the contact force acting on the surface of the object caused some deviations from the desired value, but except that peaks, the behavior is considerably similar to the result of numerical simulations. We can conclude that the proposed controller has a good performance when we use a linear actuator which has small friction.

5 Conclusion

In this article, the control system for trajectory and force control of the flexible manipulator is proposed. The proposed control system consists of feedforward controller and feedback controller. Performance of the control system for trajectory and force control has a large influence from the friction between the end of the manipulator and the surface of the object. We can conclude that by using feedforward controller and feedback controller utilizing the signals of force sensor, the proposed control system has a good performance for force control.

References

[1] A. Loria and E. Panteley, 1999, "Froce motion control of constrained manipulators without velocity measurements," IEEE Trans. on Automatic Control, 44, 7, 1407-1412

[2] B.O.Choi and K.Krishnamurthy, 1994, "Unconstrained and constrained motion control of a planar 2-link structurally flexible robotic manipulator," Journal of Robotic Systems, 11, 6, 557-571

[3] B.Siciliano, 1999, "Closed-Loop Inverse Kinematics Algorithm for Constrained Flexible Manipulators Under Gravity," Journal of Robotic Systems, 16, 6, 353-362

[4] Dai, Y.Q.,K.Usui, and M.Uchiyama, 1996, "A New Iterative Approach Solving Inverse Flexible-Link Manipulator Kinematics," Proceedings of the 35th IEEE Conference on Decision and Control, 2493-2494

[5] D.J.Latornell, D.B.Cherchas and R.Wong, 1998, "Dynamic Characteristics of Constrained Manipulators for Contact Force Control Design," International Journal of Robotics Research, Vol.17, No.3, 211-231

[6] D.W.Wang and Y.C.Soh, "Control of constrained manipulators with flexible joints," Dynamic Control, 6, 1, 33-48

[7] D.W.Wang, Y.C.Soh, Y.K.Ho et al., "Global stabilization for constrained robot motions with constraint uncertainties," Robotica, 16, 171-179

[8] F.Boyer and W.Khalil, 1998, "An Efficiant Calculation of Flexible Manipulator Inverse Dynamics," International Journal of Robotics Research, Vol.17, No.3, 282-293

[9] F.Matsuno and M.Hatayama, 1999, "Robust cooperative control of two-link flexible manipulators on the basis of quasi-static equations," International Journal of Robotics Research, Vol.18, No.4, 414-428

[10] F.Matsuno and S.Kasai, 1998, "Modelling and robust force control of constrained one-link flexible arms," Journal of Robotic Systems, 15, 8, pp.447-464

[11] H.Krishnan, 1999, "Design of force/position control laws for constrained robots, including effects of joint flexibility actuator dynamics," Robotica, 17, 41-48

[12] K.Tsuchiya, K.Tsujita and T.Kamiya, 1998 "An Inverse Model of a Manipulator with Elastic Links," Proc. of the Secont International Conference on Nonlinear Problems in Aviation and Aerospace, Vol.2, 753-760

[13] M.Moallem, R.V.Patel and K.Khorasani, 1997, "An Inverse Dynamics Control Strategy for Tip Position Tracking of Multi-Link Manipulators," Journal of Robotic Systems, 14, 9, 649-658

[14] S.B.Choi, H.B.Lee and B.S.Thompson, 1998, "Compliant Control of a Two-link Flexible Manipulator by Constraint Hamiltonian System," Mech. Mach. Teory, Vol.33, No.3, 293-306

[15] T.Yoshikawa, K.Harada, A.Matsumoto, 1996, "Hybrid Position/Force Control of Flexible-macro / Rigid-Micro Manipulator System," IEEE Trans. on Robotics and Automation, Vol.12, No.4, 633-640

[16] W.L.Xu, T.W.Yang and S.K.Tso, 1998, "Dynamic control of a flexible macro-micro manipulator based on rigid dynamics with flexible state sensing," Mechanism and Machine Theory 35, 41-53

[17] Y.C.Chang and B.S.Chen, 1998, "Adaptive tracking control design of constrained robot systems," International Journal of Adaptive Control, 12, 6, 495-526

[18] Z.X.Shi, E.H.K.Fung and Y.C.Li, 1999, "Dynamic modelling of a rigid-flexible manipulator for constrained motion task control," Applied Mathematical Modelling, 23, 509-525

[18] W.Beres and J.Z.Sasiadek, 1995, "Finite Element Dynamic Model of Multilink Flexible Manipulators," Applications in Mathematics and Computer Science, 5(2), 231,262

[20] Song and Vidyasagar, 1989, Robot Dynamics and Control, John Willey and Sons, NY

Table 1

	Body 1	Body 2	Body 3	Body 4
Length [m]	0.500	0.550	0.0276	0.120
Mass [kg]	23.70	0.426	0.444	0.288
Bending Stiffness [Nm^2]	-	0.864	-	-

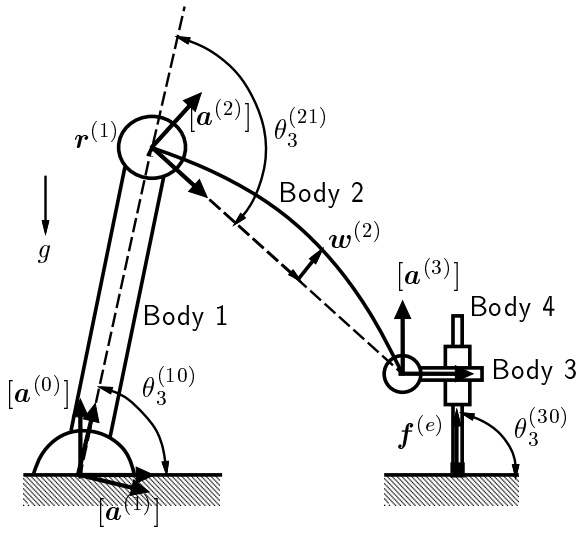

Fig. 1 Four body manipulator system

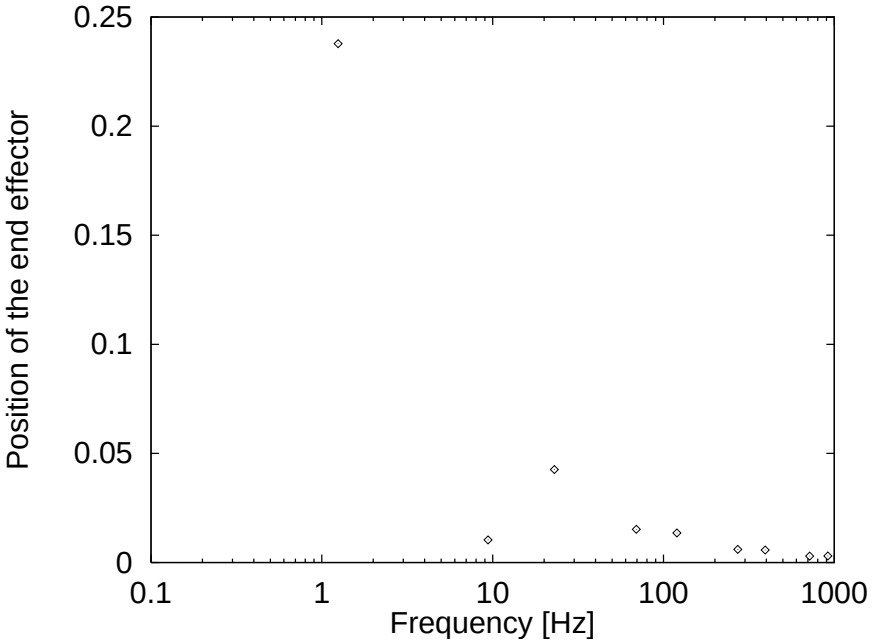

Fig. 2 Result of eigenvalue analysis

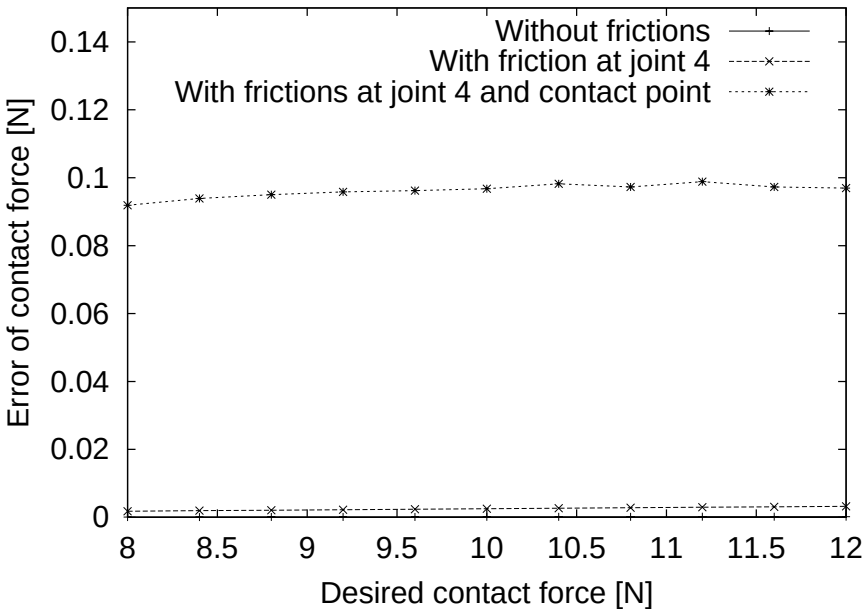

(a)

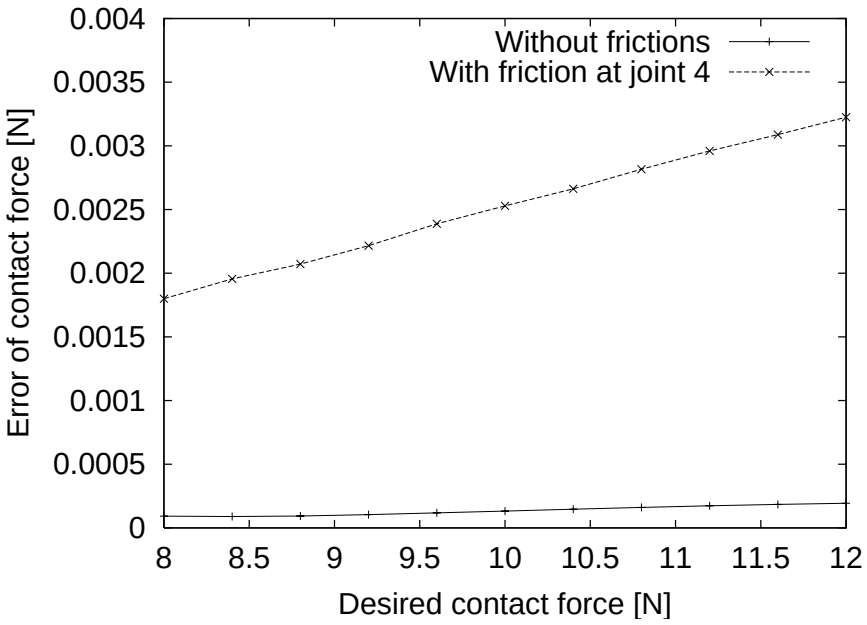

(b)

Fig. 3 Effect of frictions

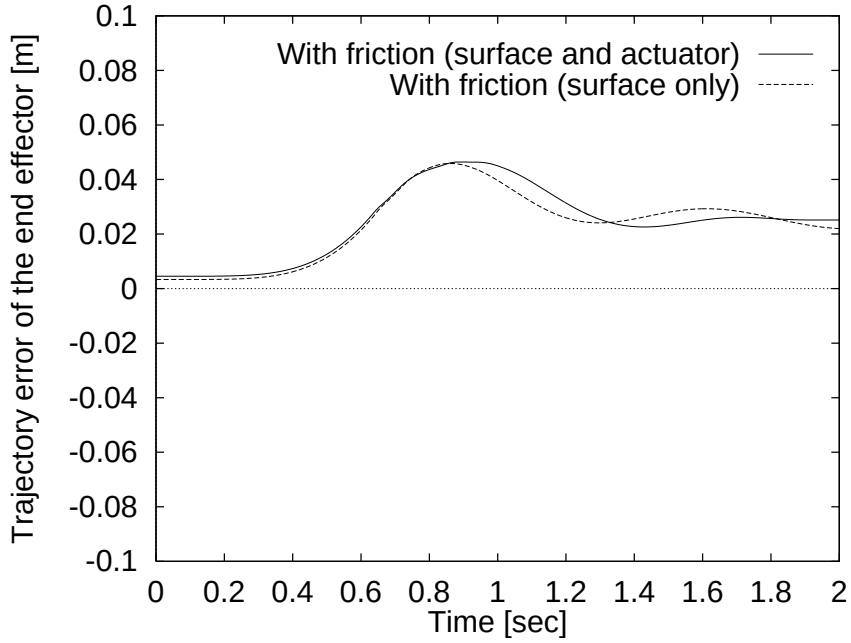

(a) Trajectory error of the end effector

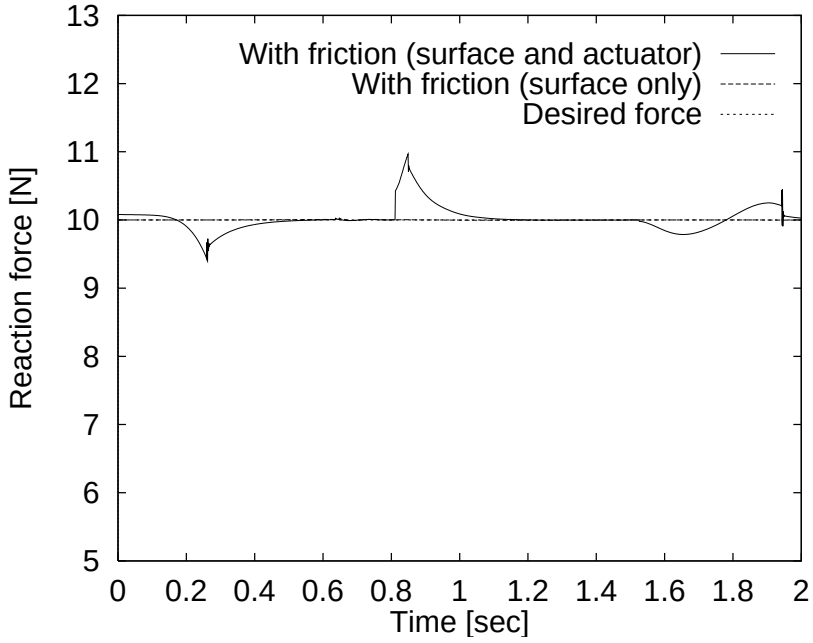

(b) The force acting on the surface

Fig. 4 CASE 1

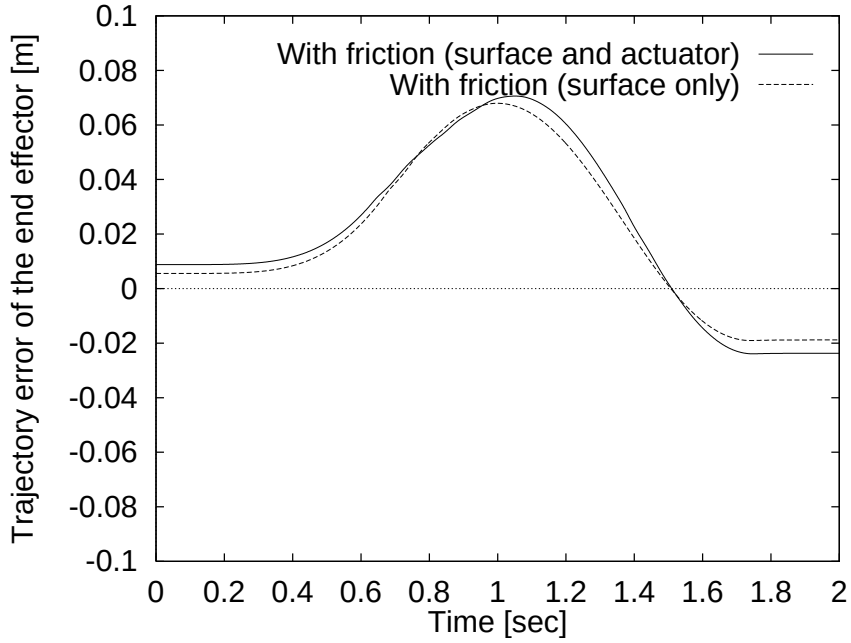

(a) Trajectory error of the end effector

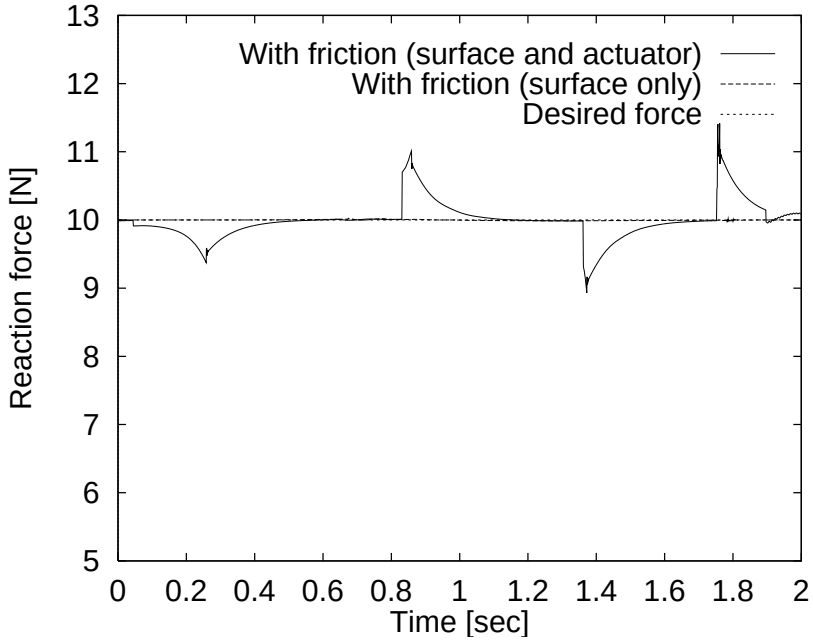

(b) The force acting on the surface

Fig. 5 CASE 2

(a)

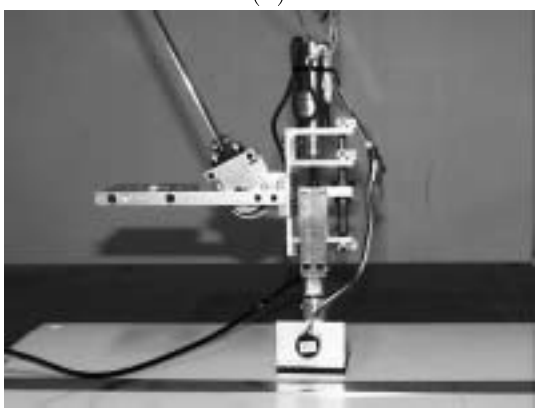

(b)

Fig.6 Hardware equipment
(a) Manipulator system
(b) End effector

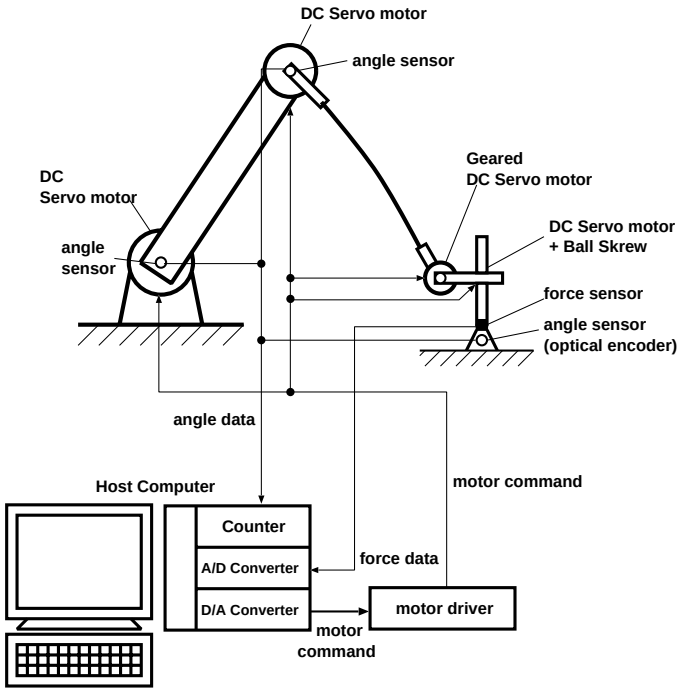

Fig. 7 Architecture of the hardware equipment

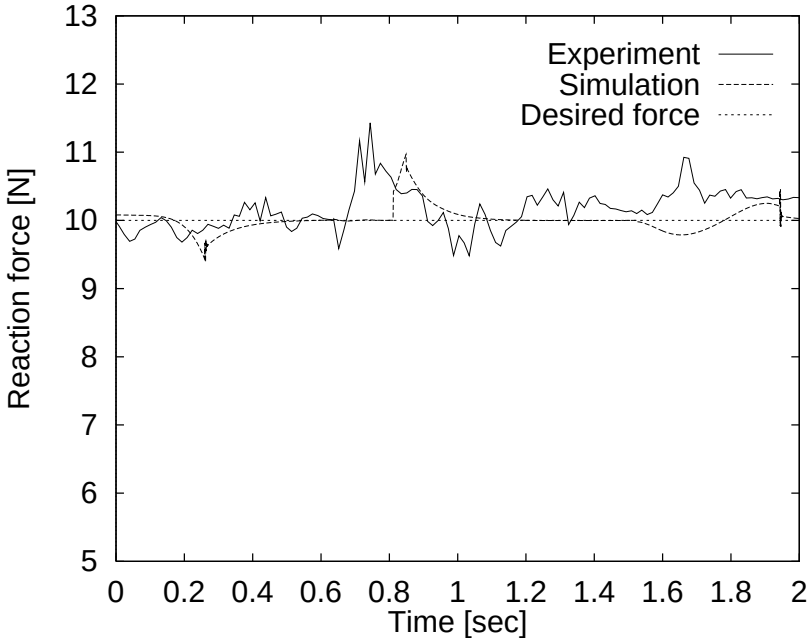

Fig. 8 Time history of reaction force (CASE 1)

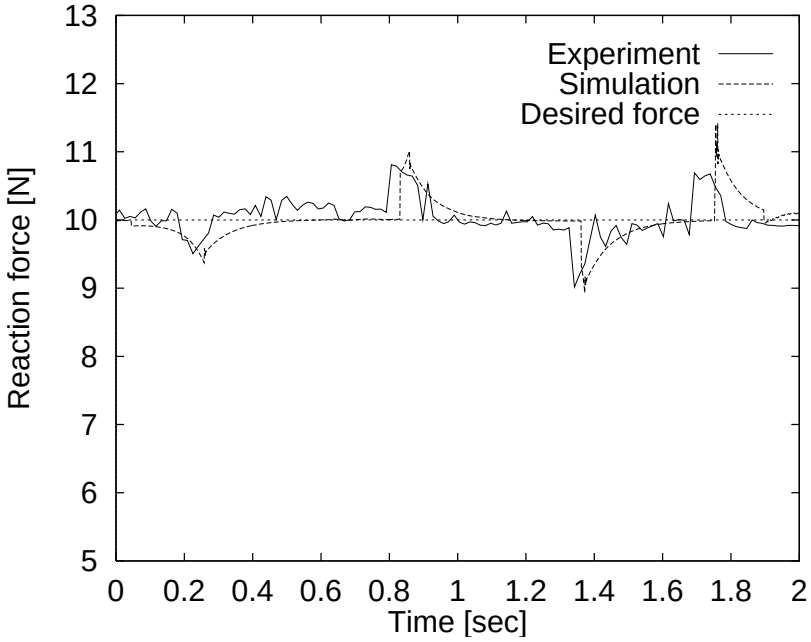

Fig. 9 Time history of reaction force (CASE 2)

A Appendix

Body 2 is divided into N finite elements which are numbered as 1, 2, $\cdots$, N from joint 2 to joint 3. The nodes are also numbered as 0, 1, $\cdots$, N from joint 2 to joint 3.

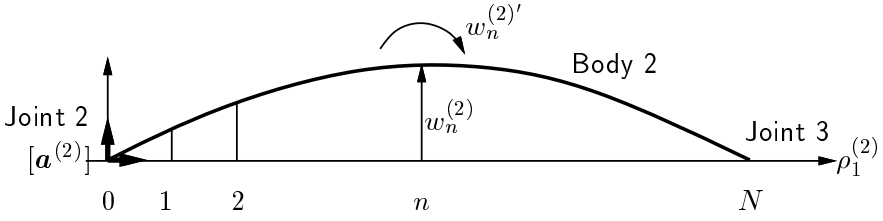

An elastic deformation in nth element, $w_{2,n}^{(2)}$, is expressed as

$$
\begin{aligned}
w_{2,n}^{(2)}(t,\rho_1^{(2)}) \;=\; & \left[x_n^0 - \frac{3}{l^2}x_n^2 + \frac{2}{l^3}x_n^3 \quad x_n - \frac{2}{l}x_n^2 + \frac{1}{l^2}x_n^3 \right. \\
& \left. \frac{3}{l^2}x_n^2 - \frac{2}{l^3}x_n^3 \quad -\frac{1}{l}x_n^2 + \frac{1}{l^2}x_n^3\right] \begin{bmatrix} \widehat{w}_{2,n-1}^{(2)}(t) \\ \widehat{w}_{2,n-1}^{\prime(2)}(t) \\ \widehat{w}_{2,n}^{(2)}(t) \\ \widehat{w}_{2,n}^{\prime(2)}(t) \end{bmatrix}
\end{aligned} \tag{27}
$$

where,

$$
\begin{aligned}
x_n \;=\; & \begin{bmatrix} 0 & ; 0 < \rho_1^{(2)} < (n-1)l \\ \rho_1^{(2)} - (n-1)l & ; (n-1)l < \rho_1^{(2)} < nl \\ 0 & ; nl < \rho_1^{(2)} \end{bmatrix} \\
l \;=\; & \frac{r_1^{(2)}}{N}
\end{aligned}
$$

$\widehat{w}_{2,n}^{(2)}$: elastic deformation at node n

$\widehat{w}_{2,n}^{\prime(2)}$: angle of rotation at node n

At nodes 0 and N, we may set the following condition;

$$\widehat{w}_{2,0}^{(2)} = \widehat{w}_{2,N}^{(2)} = 0$$

Then, an elastic deformation in body 2 is expressed as

$$w_2^{(2)}(t,\rho_1^{(2)}) = B^{(2)}(\rho_1^{(2)})\ \widehat{w}^{(2)}(t) \tag{28}$$

where,

$$
\begin{aligned}
B^{(2)} &= \begin{bmatrix} 0 \\ B_2^{(2)} \\ 0 \end{bmatrix} \\
B_2^{(2)} &= \begin{bmatrix} \widehat{b}'_1 & \widehat{b}_2 & \widehat{b}'_2 & \cdots & \widehat{b}_{N-2} & \widehat{b}'_{N-2} & \widehat{b}_{N-1} \end{bmatrix} \\
\widehat{w}^{(2)T} &= \begin{bmatrix} \widehat{w}_{2,1}^{(2)'} & \widehat{w}_{2,2}^{(2)} & \widehat{w}_{2,2}^{(2)'} & \cdots & \widehat{w}_{2,N-2}^{(2)} & \widehat{w}_{2,N-2}^{(2)'} & \widehat{w}_{2,N-1}^{(2)} \end{bmatrix}
\end{aligned}
$$